STIC-ILL

Adonis only
$20

From: Wilson, Michael
Sent: Friday, September 07, 2001 5:10 PM
To: STIC-ILL
Subject: 09/336103

TI Growth in the pre-fusion murine allantois.
AU Downs K M; Bertler C
SO ANATOMY AND EMBRYOLOGY, (2000 Oct) 202 (4) 323-31.

Michael C. Wilson
Art Unit 1633
CM1 12B05
703-305-0120

Article title	Growth in the pre-fusion murine allantois
Article identifier	0340206100009117
Authors	Downs_K_M Bertler_C
Journal title	Anatomy and Embryology
ISSN	0340-2061
Publisher	Springer
Year of publication	2000
Volume	202
Issue	4
Supplement	0
Page range	323-331
Number of pages	9
User name	Adonis
Cost centre	
PCC	$20.00
Date and time	Saturday, September 08, 2001 7:09:28 AM

Anat Embryol (2000) 202:323–331

ORIGINAL ARTICLE

Karen M. Downs · Carey Bertler

Growth in the pre-fusion murine allantois

Accepted: 26 May 2000

Abstract Prior to fusion with the chorion, the extraembryonic mesoderm of the murine (*Mus musculus*) allantois differentiates with distal-to-proximal polarity into at least two cell lineages: a chorio-adhesive cell lineage called mesothelium, and the endothelium of the umbilical vasculature. How the allantois grows is less clear, but cell proliferation and addition of mesoderm from the underlying primitive streak appear to play important roles. The aim of this study was to analyze growth in the murine allantois. Techniques of histology and microsurgery were used to examine pre-fusion allantoises at nine developmental timepoints that differed by approximately 2 h. Cell counts revealed that allantoic size increased over time. Two hours of exposure to colcemid enhanced mitotic figures, which were used to calculate the relative number of proliferating cells (mitotic index, MI) in pre-fusion allantoises at each developmental timepoint. Cell proliferation was highest in nascent allantoises and showed signs of slowing by two somite pairs. By five to six-somite pairs, when most allantoises are attaching to the chorion, the overall MI decreased significantly. No regional differences in the mitotic index were observed at any developmental stage. Total cell numbers and the mitotic index were then used to discover the extent of streak contribution to pre-fusion allantoises. Cell proliferation and streak activity were highest in nascent allantoises, after which growth occurred predominantly by cell proliferation. Formation of allantoic regenerates by microsurgical removal and culture in intact conceptuses provided independent confirmation that, as the allantois matured, the primitive streak ceased to be a major contributor to its growth. Thus, the allantois grows by both mitosis and addition of mesoderm from the streak. That the periods of highest cell proliferation and streak activity coincided raises intriguing questions concerning their interplay in the control of growth in the murine allantois.

K.M. Downs (✉) · C. Bertler
University of Wisconsin – Madison Medical School,
1300 University Avenue, Madison, WI 53706, USA
e-mail: kdowns@facstaff.wisc.edu
Tel.: 608-265-5411, Fax: 608-262-7306

Key words Colcemid · Endothelium · Mitotic Index · Placenta · Primitive Streak · Proliferation

Introduction

The chorio-allantoic placenta is formed by the union of two initially well-separated extraembryonic structures, the chorion and the allantois. The allantois is first evident as a small bud of mesoderm at the early neural plate stage (reviewed Downs 1998). Proximal epiblast, the source of allantoic mesoderm (Lawson et al. 1991), enters the posterior primitive streak at the onset of gastrulation (approximately 6.5 days postcoitum, dpc) and exits as extraembryonic mesoderm, contributing to the walls of the exocoelom and to all of the allantois. The allantoic bud grows, traverses the exocoelomic cavity, and differentiates over a period encompassing about 18 h of gestation (approximately 7.5–8.25 dpc).

The first overt sign that differentiation in the allantois is occurring is morphological: distalmost cells of the late allantoic bud (late neural plate stage) flatten to form nascent mesothelium (Downs et al. 1998). Flattened cells continue to appear as an outer rind down the length of the expanding allantois so that, by four to six-somite pairs, the entire allantoic projection is enveloped by the mesothelium. As mesothelium matures, it mediates chorio-allantoic fusion, which begins in a minority of allantoises at three to four somite pairs, and peaks by six to seven pairs (Downs and Gardner 1995).

Results of molecular and morphological analyses have revealed that, as mesothelium is forming, differentiation of core allantoic mesoderm is also underway (Downs et al. 1998). At the late neural plate stage, a few distal core cells express *flk-1*, an early marker of the endothelial cell lineage (Downs et al. 1998). Expression then spreads proximally, such that, by three to four somite pairs, large numbers of *flk-1*-expressing cells are found throughout the allantois. Morphological vascularization is evident shortly thereafter, with nascent blood vessels widespread by five to six-somite pairs.

Thus, differentiation of the allantois begins in the distal region. How differentiation relates to allantoic growth is not clear. Multiple lines of investigation suggest that the latter involves at least two major events: (1) cell proliferation (Ellington 1985), and (2) continuous addition of mesoderm from the underlying primitive streak (Beddington 1982; Copp et al. 1986; Tam and Beddington 1987; Lawson et al. 1991). In addition, the allantois may increase in size by expansion of the extracellular space between cells through the manufacture and deposition of hyaluronan (Brown and Papaioannou 1993).

Detailed analyses of spatiotemporal patterns of cell proliferation and streak activity, heretofore lacking, are critical for elucidating the genetic and developmental mechanisms of placental ontogeny. In this study, the mitotic index was determined in whole allantoises and allantoic subregions in colcemid-arrested conceptuses. The MI was used to discover: (1) the whereabouts of allantoic growth centers, (2) the coincidence of allantoic growth centers with previously documented patterns of differentiation, (3) the contribution of the primitive streak to growth in pre-fusion murine allantoises.

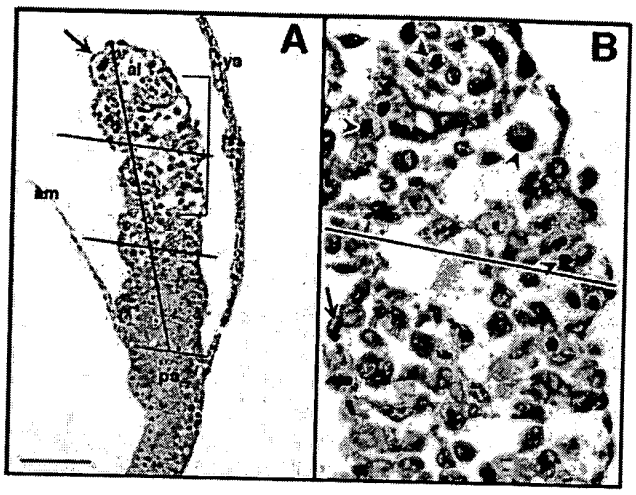

Fig. 1A,B Scoring mitotic figures. **A** Brightfield micrograph of a hematoxylin and eosin-stained sagittal section of a 6-somite-pair pre-fusion allantois (*al*) to show the relative number and the distribution of dividing cells in the three equally divided subregions, corresponding respectively to the distal (top), middle and basal (bottom) allantoic thirds. The region delineated by the vertical line to the right of the allantois is enlarged in **B**. **B** Examples of colcemid-arrested mitotic figures are shown (*arrowheads*). *Arrows* in **A** and **B** point to mesothelial cells (*am* amnion, *ps* primitive streak, *ys* yolk sac). *Bar* in **A**: 150 μm (**A**); 75 μm (**B**)

Materials and methods

Mice used

Care and use of laboratory animals for this study were in accordance with the University of Wisconsin Institutional Animal Care and Use Committee and the Guide for the Care and Use of Laboratory Animals (National Institute of Health publication 85-23, revised 1985). F1 hybrids of the genetic background (C57BL/6 x CBA), maintained under light-reversed conditions (dark period: 13.00–1.00), were mated. Pregnant females were killed by cervical dislocation between 7.5 and 8.5 days postcoitum (dpc); the uterine horns were placed in phosphate-buffered saline (PBS; Sigma) and the uterine muscles were dissected away from the decidua. The F2 conceptuses were dissected out of the decidua in DMEM-based dissection medium (Lawson et al. 1986; Downs and Gardner 1995) and staged either according to Downs and Davies (1993) or by numbers of somite pairs. Developmental stages used in this study encompassed the neural plate/early allantoic bud through six-somite pair stages; only conceptuses in which the allantois had not yet fused with the chorion were used. Passage from one morphological stage to the next takes approximately 2 h in culture (Downs and Gardner 1995). Embryos at one-somite pair were excluded from the study, as this developmental timepoint was difficult to ascertain in the dissection microscope. Thus, the interval between the late headfold and two-somite pair stages was about 4 h.

Colcemid arrest, histology and mitotic index

In three experiments, six conceptuses from each of nine midgastrula stages (Early Neural Plate/Early Bud (EB); Late Neural Plate/Late Bud (LB); Early Headfold, EHF; Late Headfold, LHF; two to six-somite pairs) were divided into pairs. Each member of the pair was cultured in 1 ml of culture medium (Lawson et al. 1986; Downs and Harmann 1997) either in the absence or presence of colcemid (demecolcine, Sigma, D7385; final concentration: 0.01 μg/ml) for 2 h. Colcemid was used for two reasons. First, enrichment of mitotic figures by colcemid would minimize standard errors due to small sample size. Second, optimization of mitotic figures was necessary for accurate determination of streak contribution to allantoic growth. Exposure to colcemid was carried out for 2 h, as this period had already been used in the rat (Ellington 1985). Moreover, 2 h is the time it takes for conceptuses to pass from one morphological stage to the next (Downs and Davies 1993; Downs and Gardner 1995). Thus, for any given 2-h labeling interval, conceptuses will have passed to the next developmental stage and the number of metaphase-arrested cells would reflect cell proliferation for that 2-h interval. In preliminary experiments, 0.01 μg/ml colcemid achieved maximal enrichment of mitotic figures and maintained tissue integrity and viability. Less colcemid (0.001 μg/ml) produced little enrichment, whereas more colcemid (0.1 μg/ml) produced levels of enrichment similar to 0.01 μg/ml, but also marked tissue necrosis (data not shown).

After culture, conceptuses were rinsed five times in DMEM-based dissection medium, then twice in PBS, and fixed for 1 (neural plate – three-somite pairs) or 2 h (four to six-somite pairs) in Bouin's fluid (Kaufman 1992) at room temperature. After three 20-min rinses in PBS, conceptuses were embedded in paraffin according to standard protocols of dehydration and clearing (e.g., Kaufman 1992). Conceptuses were sectioned at 6 μm, dewaxed, stained in hematoxylin (Gill's no. 1, Sigma) and eosin, mounted in Surgipath (Richmond, Ill.) and cover-slipped.

Every section containing allantoic tissue was photographed onto Ektachrome T160 film, scanned, and projected onto the computer screen. Between the neural plate/late allantoic bud and 6-somite pair stages, allantoises were subdivided into three regions, basal, middle and distal thirds, as previously described (Downs et al. 1998; Fig. 1). The neural plate/early allantoic bud did not undergo this procedure, as it was too small to be meaningfully subdivided. Metaphase and non-metaphase nuclei, which were taken to be representative of whole cells, were counted in allantoic sections separated by 12 μm. Average cell numbers from pooled colcemid-treated (n=3) and pooled untreated (n=3) conceptuses for each developmental timepoint were calculated separately. The MI was also calculated separately in pooled treatment groups at each developmental timepoint; it was defined as the ratio of mitotic figures to the total number of nuclei in each allantois or allantoic subregion, which was then multiplied by 100. Statistical analyses using the Student's two-way t-test (Mini-Tab, equal

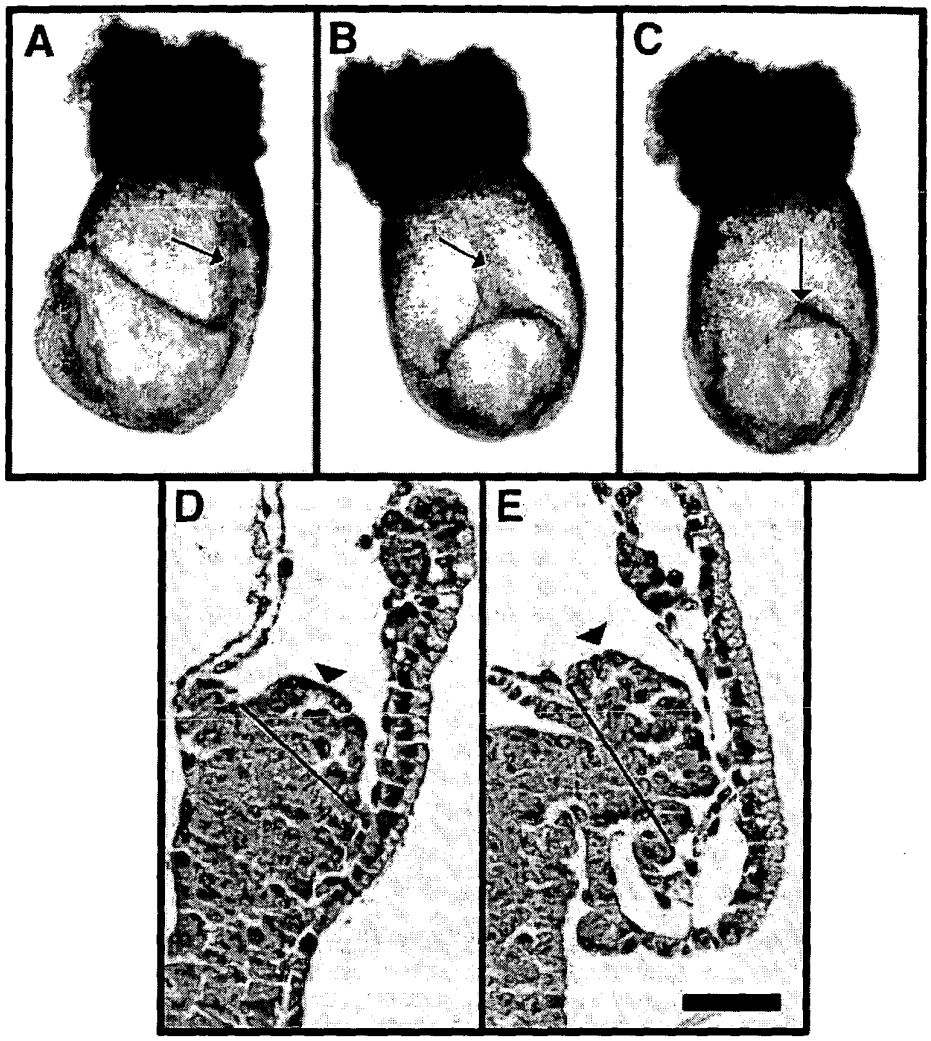

Fig. 2A–E Allantoic regenerates. Headfold-stage conceptus, side- (**A**) and posterior (**B**) views before removal of the allantois (**C**), indicated by *arrows*. Regenerated allantoises (*arrowheads*) at the early–late headfold **D** and 5–6-somite-pair intervals **E**. Based on examination of a series of immediately-fixed operated conceptuses (n=12), regenerated cells were taken as those above the computer-generated lines. *Bar* in **E**: 338 μm (A–C), 40 μm (**D**, **E**)

variances assumed, Confidence Interval = 95.0%, "pooled" subcommand) determined significant differences ($P< 0.05$) between each treatment category at each developmental timepoint for both cell numbers and the mitotic index.

Allantoic regenerates

After dissection and staging conceptuses, allantoises were microsurgically removed ("operated" conceptuses) as previously described (Downs and Gardner 1995; Fig. 2A–C). Control and operated conceptuses were cultured alongside each other for 2 h (Downs and Gardner 1995), after which all conceptuses were prepared for histology. After dewaxing, 6 μm sections were stained in hematoxylin/eosin, cover-slipped, and examined in the compound microscope. The two lowest allantoic insertion points between the yolk sac and amnion (Downs and Harmann 1997; Downs et al. 1998) were determined and regenerated nuclei were counted in every third section above this point (Fig. 2D, E) as described in the previous section. The numbers of regenerated cells were pooled at each developmental timepoint and the average was taken.

Results

Cell numbers and the MI in whole allantoises and allantoic subregions

Cells were counted in allantoises (Table 1). Colcemid had no adverse effect on cell numbers, either in whole allantoises or in allantoic subregions ($P >0.05$, data not shown). On the basis of these findings, control and colcemid-arrested embryos were pooled to obtain average cell numbers at each developmental stage (Table 1). The relative change in allantoic cell numbers was calculated at all successive developmental intervals (Table 1, Fig. 3). Cell numbers generally increased in both whole allantoises and allantoic subregions with increasing developmental age. The base typically contained the highest cell numbers, and the distal third the least. Growth in whole allantoises and allantoic subregions was maximal between the headfold and two-somite pair stages, after which it slowed. Increased deposition of extracellular

Table 1 Average cell numbers and mitotic indices in pre-fusion allantoises. Total cell numbers and mitotic indices were calculated in (1) whole allantoises between the early neural plate/early allantoic bud (EB) and 6-somite pair stages, and (2) allantoic sub-regions between the late neural plate/late allantoic bud (LB) and 6-somite pair stages in 3 untreated and 3 colcemid-treated allantoises for each developmental stage. Because no significant differences ($P \geq 0.05$, see Materials and Methods) were found in total cell numbers at any developmental stage between colcemid-treated and untreated allantoises, total cell numbers were pooled and averaged in this Table ($n=6$). In contrast, the mitotic indices of colcemid-treated conceptuses contained signficantly higher MIs (≥EHF stages) than untreated conceptuses so data from colcemid-treated embryos only are shown in this Table ($n=3$). The relative changes in cell number with increasing developmental age are plotted in Fig. 3 and the mitotic indices in Fig. 5 (*EHF* early headfold, *LHF* late headfold, 2–6-s, 2–6-somite pairs, *s.e.m.* standard error of the mean, *N/A* not applicable, *ND* not done

Stage	Average cell number±S.E.M. (MI±S.E.M.)				Percent change in cell number from preceding stage			
	Whole	Basal Third	Mid-Third	Distal Third	Whole	Base	Mid	Distal
EB	303±45 (10.0±1.1)	ND	ND	ND	N/A	N/A	N/A	N/A
LB	389±27 (15.8±1.5)	196±11 (16.2±1.6)	134±15 (15.6±2.6)	60±5 (16.1±1.4)	22.1	ND	ND	ND
EHF	714±84 (20.7±0.7)	368±44 (20.2±0.7)	245±35 (20.8±1.7)	101±11 (22.1±3.3)	45.5	46.6	45.3	40.9
LHF	1227±120 (18.4±5.2)	784±85 (17.4±4.6)	341±22 (18.8±6.0)	156±16 (22.2±6.3)	41.8	53.1	28.3	35.3
2-s	2597±232 (10.1±0.5)	1407±146 (10.9±0.6)	790±55 (9.5±1.0)	401±55 (10.2±1.9)	47.6	40.9	54.3	57.7
3-s	3131±296 (9.4±0.6)	1652±121 (9.8±1.0)	922±95 (8.9±0.6)	557±12 (9.5±1.9)	17.1	14.8	14.3	28.0
4-s	3399±246 (10.1±0.5)	1852±96 (10.3±0.1)	1040±119 (10.5±1.2)	507±62 (9.5±1.1)	7.9	10.8	11.4	–9.9
5-s	3847±308 (7.7±0.8)	1991±169 (7.7±0.8)	1225±113 (7.4±0.7)	631±98 (8.2±1.4)	11.6	7.0	20.2	19.7
6-s	4224±150 (6.9±0.5)	2144±87 (7.1±0.3)	1403±65 (7.1±0.7)	676±64 (6.3±0.8)	8.9	7.2	7.1	6.6

matrix ("distal cavitation") may be responsible for the negative number in the distal region at four-somite pairs (Fig. 3), reducing cell-cell contacts and forcing translocation of some tip cells into the mid-region (compare Fig. 4A and B). Although not quantified, apoptotic figures were rare at all timepoints.

Next, mitotic indices were calculated. Comparison of MI's between colcemid- and untreated allantoises revealed that metaphase arrests were enriched approximately 2-fold in treated allantoises and were significantly higher than those in untreated ones at most developmental stages (Table 1, Fig. 5A). Because the trends in cell proliferation were similar in treated and untreated allantoises (Fig. 5A), colcemid enrichment contributed little to understanding cell proliferation. Nonetheless, enhanced numbers of metaphase arrests would be required to estimate the streak contribution to allantoic growth (next section); thus, only colcemid-treated allantoises were used in the remainder of the study.

Mitotic indices encompassed both the outer and inner allantoic cell populations, peaking at the headfold stages, but falling by two-somite pairs (Fig. 5A). Owing to the imbalance between 2 h of exposure to colcemid and the 4-h difference between the late headfold and two-somite pair stages, the MI at the late headfold stage may be an underestimate of the true index. At five-somite pairs, the MI dropped significantly (Fig. 5A). To discover whether any allantoic region was more proliferative than others, the MI was calculated for each subregion at all but the early allantoic bud stage (see Materials and Methods). No significant differences were found in the MI for any region at any developmental stage (Fig. 5B).

Allantoic growth from the posterior primitive streak

Potency experiments in advanced blastocysts demonstrated that the allantois is derived from primitive ectoderm, or epiblast (Gardner et al. 1985). Clonal fate mapping further revealed that, during gastrulation, a portion of the proximal epiblast that ingresses into the posterior primitive streak emerges as allantoic mesoderm (Lawson et al. 1991). The streak continues to contribute to the allantois during the early somite stages (Tam and Beddington 1987).

To discover the contribution of the primitive streak to allantoic growth, the number of proliferating cells at each developmental timepoint (Table 2) was subtracted from the total number of new cells formed during successive intervals (Table 1). Given that pre-fusion allantoises have no other external source of cells, those cells not derived from cell proliferation were considered to be generated by the posterior streak.

Comparison of intrinsic and extrinsic cell contributions to the allantois (Fig. 6) revealed that the streak made its largest contribution to allantoic growth between

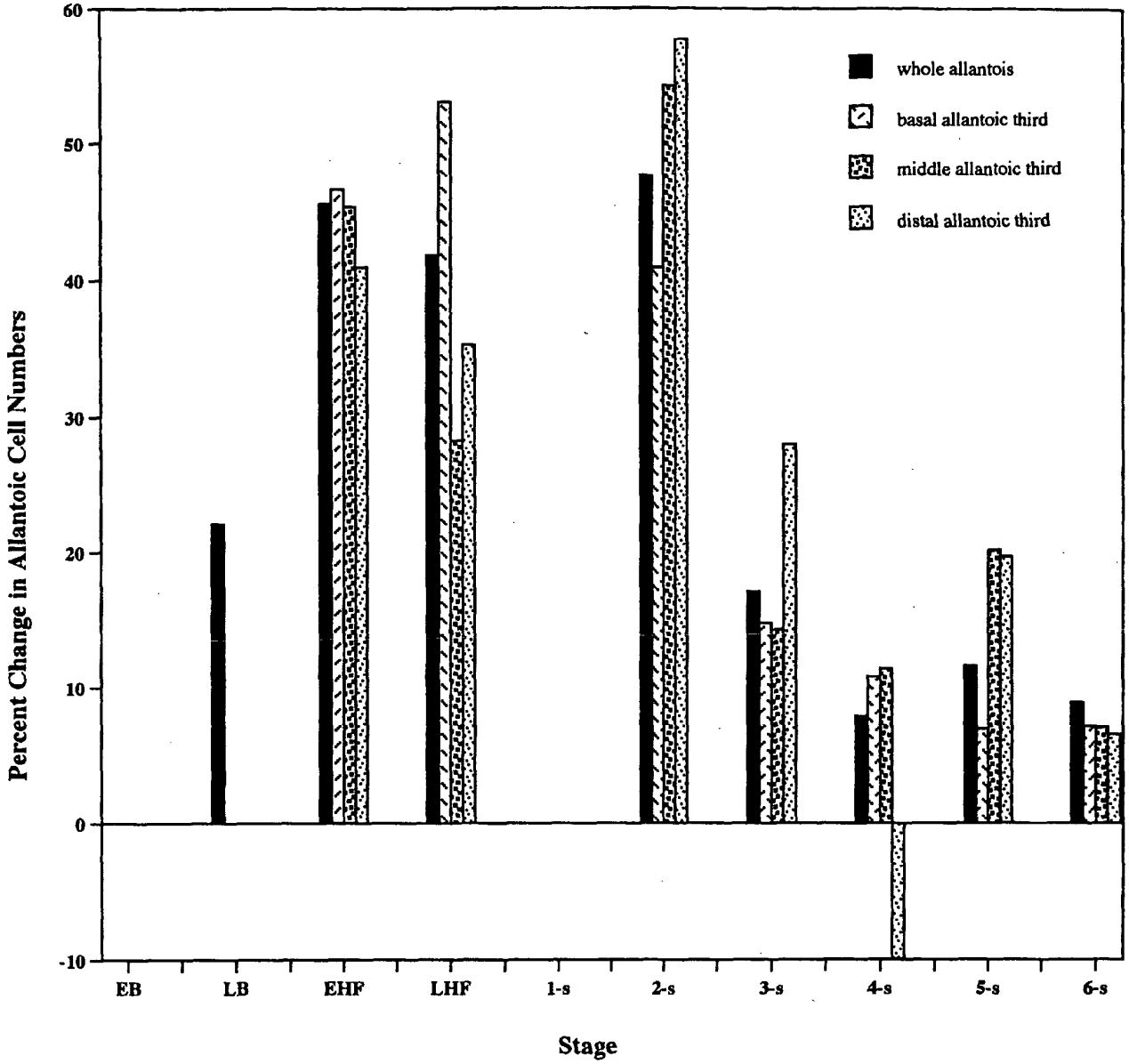

Fig. 3 Relative change in allantoic cell numbers at 2-h developmental intervals. Average allantoic cell numbers (Table 1) were compared at 2-h intervals and the percent change for each interval plotted. Abbreviations as in Table 1

the neural plate and headfold stages. By two-somite pairs, cell proliferation and the primitive streak were approximately equal contributors but, by three-somite pairs, subsequent allantoic growth occurred primarily by cell proliferation.

Allantoic regeneration

The prediction that highest and lowest streak activity occurred at early and later somite stages, respectively, was tested by microsurgically removing allantoises (Downs and Gardner 1995; Fig. 2A–C) and examining allantoic regeneration over a 2-h period. Operated and control conceptuses were cultured alongside each other for 2 h, after which the numbers of cells in regenerated allantoises were counted after histological preparation. Originally, unoperated control conceptuses were included in this part of the study to determine by gross visualization the increase in allantoic size at each time interval. However, owing to the semi-opacity of the yolk sac, and the possibility that gross allantoic measurements could therefore be inaccurate, control conceptuses had little value other than ensuring non-toxicity of culture. Cell counts in the allantoic regenerates were remarkably similar to the predicted numbers of streak-derived cells at all developmental intervals (Fig. 7). Thus, allantoic regener-

Table 2 Origin of new cells in pre-fusion allantoises. The total number of new allantoic cells (column 2) for each developmental interval (column 1) was taken from Table 1. The MI of colcemid-exposed allantoises (Table 1) was used to calculate (MI×total cell number at same stage) the number of new cells added to allantoises at each developmental timepoint by cell proliferation (column 3). This number was subtracted from the total number of new cells to estimate the proportion of these that had been added to the allantois from the primitive streak (column 4).

Interval	No. cells added to allantois in this interval (observed)	No. cells (% of total) contributed by cell proliferation (calculated)	No.cells (% of total) contributed from the primitive streak (calculated)
EB/LB	86	30.6 (35.6%)	55.4 (64.4%)
LB/EHF	325	61.5 (18.9%)	263.5 (81.0%)
EHF/LHF	513	147.8 (28.8%)	365.2 (71.2%)
LHF/2-s	1370	225.8 (16.5%)	1144.2 (83.5%)
2-/3-s	534	262.3 (49.1%)	271.7 (50.9%)
3-/4-s	268	294.3 (100%)	0[a] (0)
4-/5-s	448	343.3 (76.6%)	104.7 (23.4%)
5-/6-s	377	296.2 (78.6%)	80.8 (21.4%)

[a] Given the potentially wide range of new cells added to whole allantoises at 3-/4-somite pairs (Table 1, calculated), the amount of streak-derived mesoderm may be higher than zero. In accordance with this possibility, the observed mean number of regenerated cells counted for this interval was 71.2 (Fig. 7)

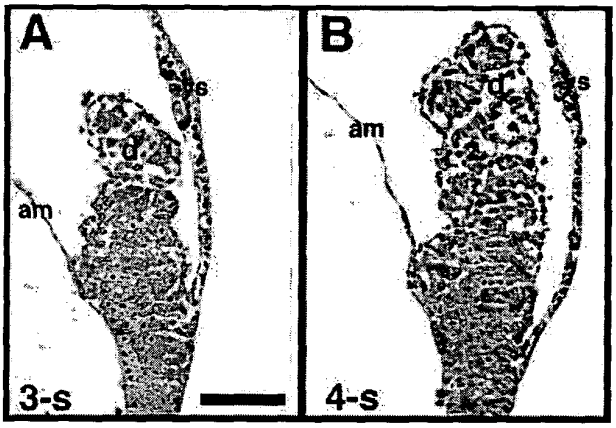

Fig. 4A, B Distal cavitation at 3–4-somite pairs. Brightfield micrographs of hematoxylin/eosin-stained histological sections of (**A**) 3-somite pair allantois, and (**B**) 4-somite pair allantois to illustrate increasing extracellular space (distal cavitation) between allantoic cells in the distal (*d*) allantoic region. *Bar* in **A**: 100 μm

ates validated the accuracy of cell counts, mitotic indices and the periods of greatest streak activity.

Discussion

A previous study in the rat had demonstrated that the allantois increases in size by cell proliferation and distal cavitation (Ellington 1985). Fate mapping studies in the mouse revealed that the murine allantois originates in proximal epiblast which, after translocation through the posterior primitive streak, is deposited into the expanding exocoelom as extraembryonic mesoderm (Beddington 1982; Copp et al. 1986; Lawson et al. 1991). Extraembryonic mesoderm contributes a cell layer to the chorion, yolk sac, and amnion, and to all of the allantois. Later studies suggested that the posterior streak continues to be active in growth of the allantois through early somite stages (Tam and Beddington 1987; Downs and Gardner 1995).

In this study, we set out to examine general trends of cell proliferation in the maturing murine allantois, our initial goal being to relate those trends to what is currently known about differentiation in this organ. The stages examined represented about 18 h of development and encompassed the time when the allantois first appears as a bud, expands in size and traverses the exocoelomic cavity, just prior to fusion with the chorion. We first established that the allantois increased in size by addition of new cells. At all developmental stages, the basal third typically contained the highest cell number, and the distal third the least (Table 1, Fig. 3). At one developmental timepoint (four-somite pairs), the distal region appeared to lose cells. It is unlikely that loss was due to cell death, as this had not previously been observed in the rat during the equivalent time period (Ellington 1985) nor were conspicuous deaths observed in this study. Rather, cell diminution could be attributed to regressive cell movement into the mid-region as a result of distal cavitation, or increased secretion of extracellular matrix in the distal third (Ellington 1985; Fig. 4, this study).

Evaluation of the MI demonstrated that cell proliferation peaked in the allantois during the headfold stages, but showed evidence of declining by two-somite pairs. By five to six-somite pairs, the MI reached its lowest rate.

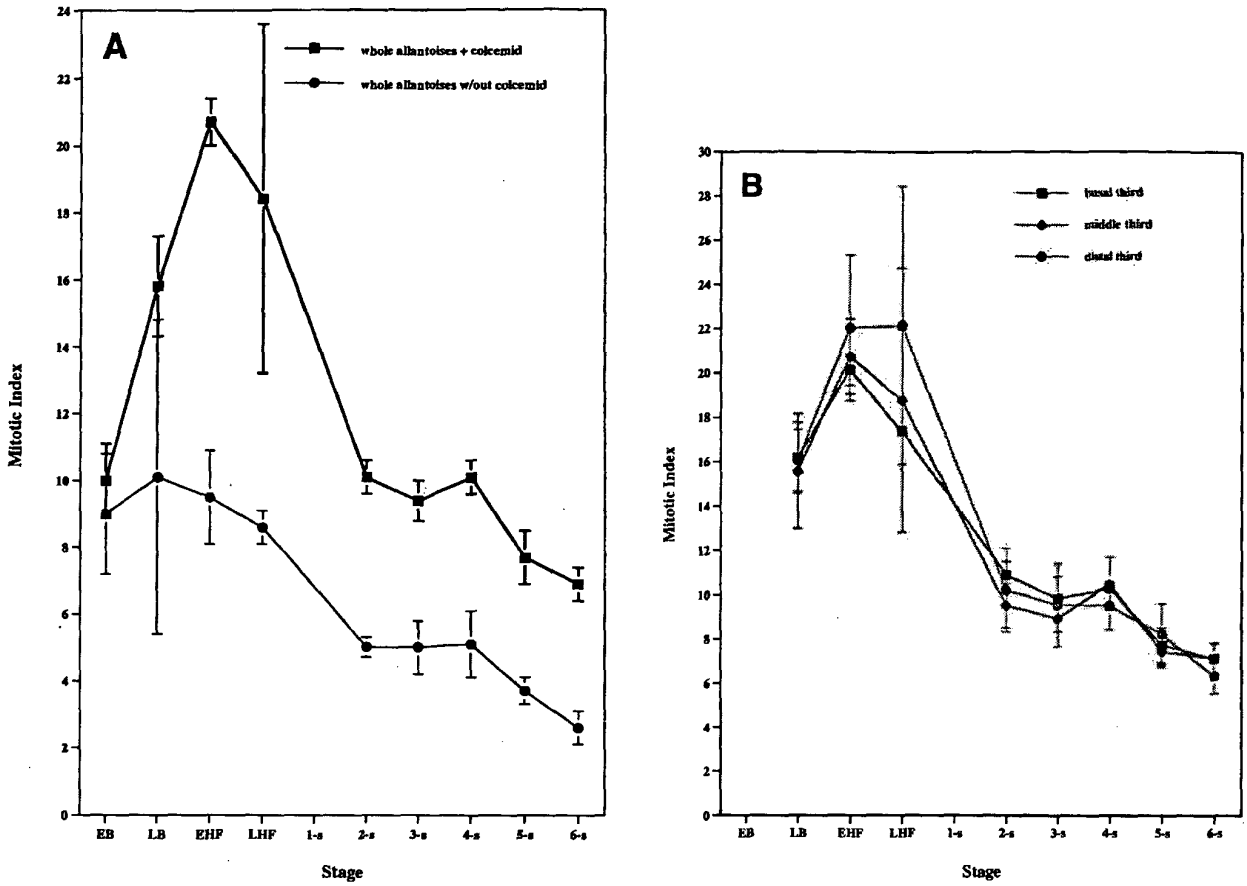

Fig. 5A, B Mitotic index (MI) in pre-fusion allantoises as a function of developmental stage. For each developmental stage, the average MI in untreated and colcemid-treated allantoises was calculated as the total number of metaphase-arrested nuclei over the total number of nuclei for each of three colcemid-treated or untreated allantoises, and the ratio then multiplied by 100. A Student's *t*-Test (see Materials and Methods) demonstrated significant differences in colcemid enrichment between untreated and colcemid-arrested allantoises at developmental stages ≥EHF (data not shown). **A** MI, whole allantoises. *P*-values of the MI for each developmental interval in colcemid-treated conceptuses: EB-LB, 0.99; LB-EHF, 0.09; EHF-LHF, 0.69; LHF–2-s, 0.18; 2–3-s, 0.43; 3–4-s, 0.37; 4–5-s, 0.06; 5–6-s, 0.79. **B** MI, allantoic subregions. *P*-values were greater than 0.05 between subregions at each developmental stage. See Materials and Methods for details. Standard errors of the mean are shown for the MI at each developmental stage. Abbreviations as in Table 1

Similar to previous findings in the rat (Ellington 1985), there were no regional differences in the MI at any developmental stage. The decline in MI accorded with attenuation of expression of the *c-myc* proto-oncogene in the allantois with increasing developmental ages (Downs et al. 1989). *c-myc*, whose target genes may include cdc25A, cyclin A, and cyclin E (Dang 1999), is thought to play an important role in control of the cell cycle.

Why the MI was initially high but decreased markedly by two-somite pairs is unclear. One possibility is that, similar to other developing cell lineages (e.g., Raff et al. 1998; Malavel et al. 1999), differentiation and cell proliferation may be inversely related in the allantois. This possibility is supported by previous observations that revealed that, between two- and six-somite pairs, widespread vascularization takes place in allantoises as they also become competent to fuse with the chorion (Downs and Gardner 1995; Downs et al. 1998).

Alternatively, the initial increase in cell proliferation could be due to the deposition of hyaluronan, an extracellular matrix proteoglycan secreted by mesoderm, including the allantois, as it forms during gastrulation (Brown and Papioannou 1993; K. Downs, unpublished observations). Hyaluronan has long been implicated in the regulation of embryonic morphogenesis. Owing to its hydrophilic nature, secretion of hyaluronan decreases contact-inhibited growth, thereby permitting cell proliferation (reviewed Toole 1981, 1990). Moreover, changes in cell shape, especially to a flattened fibroblastic form as found in the developing allantois (Ellington 1985), have been shown to lead to more rapid growth and greater incorporation of [^{3}H]-thymidine (e.g., Glowacki et al. 1983). However, given that hyaluronan facilitates cell proliferation, it is not clear why the mitotic index declined in allantoises at two-somite pairs. From that point on, intercellular spacing between allantoic cells appeared to be enhanced (see Downs et al. 1998, Figs. 2 and 3 for examples).

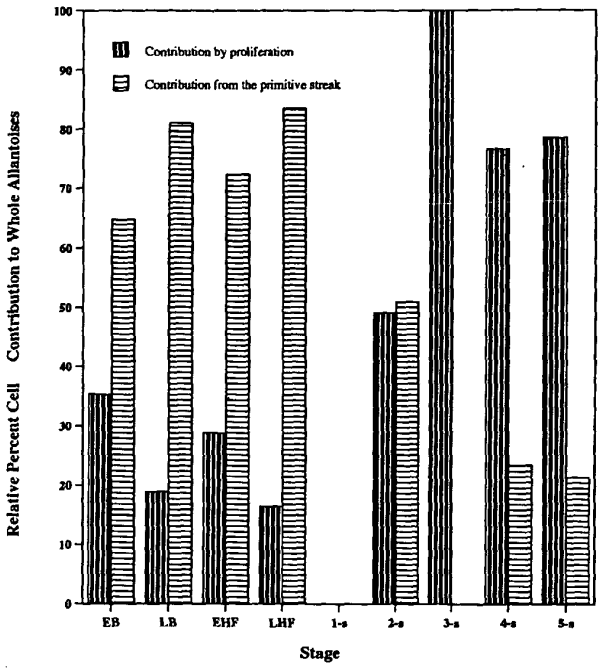

Fig. 6 Relative cell contribution to whole allantoises. Data from Table 2 were plotted in this column graph. The relative contributions of new cells to whole allantoises by cell proliferation and the posterior primitive streak are represented between the early neural plate and 6-somite pairs stages. Abbreviations as in Table 1

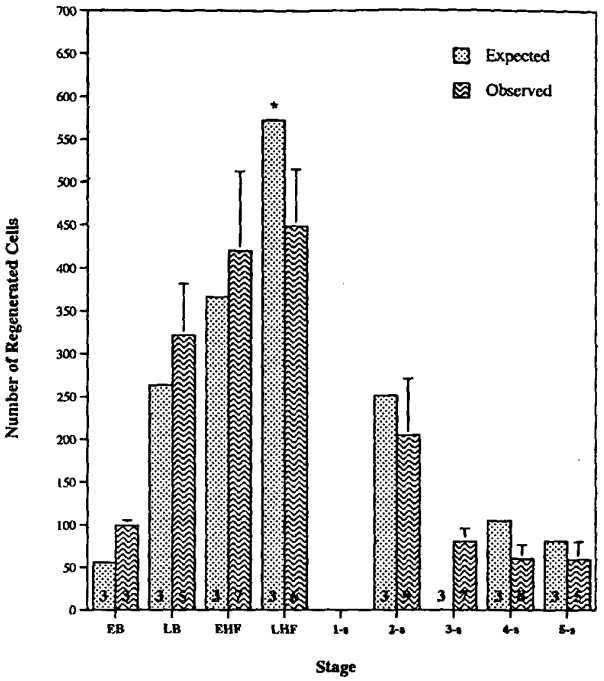

Fig. 7 Cell numbers in allantoic regenerates. Operated conceptuses were prepared for histology and cell numbers counted in the regenerates ("Observed"). "Observed" numbers were plotted against the calculated number of streak-derived cells in Table 2. The *asterisk* over "LHF" indicates that, because the predicted number of regenerated cells encompassed the LHF–2-somite pair 4-h interval (see Materials and Methods), this number was arbitrarily halved

Part of the answer may lie with the primitive streak, whose greatest contribution to the allantois during the headfold stages coincided with the period of highest mitotic activity. At two-somite pairs, cell proliferation and the primitive streak contributed equally to allantoic growth but, thereafter, both declined, with cell proliferation sustaining relatively modest allantoic growth.

The mechanism by which the streak may be involved in the control of cell proliferation is not known. Indeed, the primitive streak is one of the most important, yet least understood, structures in the embryonic development of birds and mammals (reviewed Bellairs 1986). Its role, like that of the amphibian blastopore, is to enable epiblast to pass through and become mesoderm and endoderm. Thus, one explanation for streak involvement in proliferation may be mechanical, with vigorous epiblast movement through the streak forcing growth pressure in the allantois to the point where allantoic cells are stretched, change shape, and growth is stimulated. Together with hyaluronan, the streak may provide mechanical stress while hyaluronan reduces cell-cell contacts. Then, as the streak ceases activity, cells may further change shape, growth slows and gene activity becomes focused on differentiation.

An alternative possibility for streak involvement in allantoic cell proliferation may be that streak-derived mesoderm expresses growth factors critical for allantoic proliferation (reviewed Boucher and Pedersen 1996). For example, BMP-4, a member of the TGFß superfamily of secreted polypeptide molecules, is localized to the posterior primitive streak and extraembryonic mesoderm, including the allantois, during gastrulation (Winnier et al. 1995). Perhaps, as mesodermal cells are pushed into the allantois, they bring with them growth factors that are both self-stimulatory and that induce high levels of proliferation in surrounding cells. Then, as epiblast movement through the streak slows down, fewer stimulatory cells enter the allantois, fewer cells maintain required amounts of growth factor expression, and the mitotic index decreases.

Two key observations made in this study support but do not distinguish between these fascinating hypotheses. First, the proportion of streak-generated allantoic cells was quite high between the late allantoic bud and late headfold stages (Table 2). During this time, streak activity may have imparted mechanical stress and/or provided enough growth factors via the formation of mesoderm to sustain the high levels of proliferation observed throughout the allantois. Second, as streak activity slowed, the proportion of new cells added to the allantois correspondingly decreased. According to the aforementioned hypotheses, cessation of streak activity would have brought with it less mechanical tension and fewer growth factors, leading the MI to its lowest point (Table 1, Fig. 5).

As in all developing systems, understanding the relationship between cell growth and differentiation poses an enormous challenge. Correct placentation is critical for the sustained survival and health of all eutherian mammals. Elucidation of the genetic and developmental control of placental ontogeny is therefore of fundamental importance in embryogenesis. The classical approaches used here to discover how the allantois grows provide a sound framework for future studies designed to examine the multifactorial control of proliferation and differentiation of extraembryonic allantoic mesoderm.

Acknowledgements The authors are grateful to Shannon Gifford for help with the initial computer analysis, to Yanira O. Naumann and Jacalyn McHugh for technical assistance, to Professor Richard Gardner for reading an early draft of the manuscript, and to Professor Andrew Copp and the two anonymous reviewers for their generous comments on the data. This work was supported by the National Institutes of Health to K. M. D. (1-R29-HD36847-01) and the Parke-Davis Atorvastatin Research Foundation (K.M.D.).

References

Beddington RSP (1982) An autoradiographic analysis of tissue potency in different regions of the embryonic ectoderm during gastrulation in the mouse. J Embryol Exp Morphol 69:265–285

Bellairs R (1986) The primitive streak. Anat Embryol 174:1–14

Boucher DM, Pedersen RA (1996) Induction and differentiation of extra-embryonic mesoderm in the mouse. Reprod Fertil Dev 8:765–777

Brown JJ, Papaioannou VE (1993) Ontogeny of hyaluronan secretion during early mouse development. Development 117:483–492

Copp AJ, Roberts HM, Polani PE (1986) Chimaerism of primordial germ cells in the early postimplanation mouse embryo following microsurgical grafting of posterior primitive streak cells in vitro. J Embryol Exp Morphol 95:95–115

Dang CV (1999) c-Myc target genes in cell growth, apoptosis, and metabolism. Mol Cell Biol 19:1–11

Downs KM (1998) The murine allantois. Curr Top Dev Biol 39:1–33

Downs KM, Davies T (1993) Staging of gastrulation in mouse embryos by morphological landmarks in the dissection microscope. Development 118:1255–1266

Downs KM, Gardner RL (1995) An investigation into early placental ontogeny: allantoic attachment to the chorion is selective and developmentally-regulated. Development 121:407–416

Downs KM, Harmann C (1997) Developmental potency of the murine allantois. Development 124:2769–2780

Downs KM, Martin GM, Bishop JM (1989) Contrasting patterns of *myc* and *N-myc* expression during gastrulation of the mouse embryo. Genes Dev 3:860–869

Downs KM, Gifford S, Blahnik M, Gardner RL (1998) The murine allantois undergoes vasculogenesis that is not accompanied by erythropoiesis. Development 125:4507–4521

Ellington SKL (1985) A morphological study of the development of the allantois of rat embryos in vivo. J Anat 142:1–11

Gardner RL, Lyon MF, Evans EP, Burtenshaw MD (1985) Clonal analysis of X-chromosome inactivation and the origin of the germ line in the mouse embryo. J Embryol Exp Morph 52: 141–152

Glowacki J, Trepman E, Folkman J (1983) Cell shape and phenotypic expression in chondrocytes. Proc Soc Exp Biol Med 172:93–98

Kaufman MH (1992) The Atlas of Mouse Development. London: Academic Press

Lawson KA, Meneses JJ, Pedersen RA (1986) Cell fate and cell lineage in the endoderm of the presomite mouse embryo, studied with an intracellular tracer. Dev Biol 115:325–339

Lawson KA, Meneses JJ, Pedersen RA (1991) Clonal analysis of epiblast fate during germ layer formation in the mouse embryo. Development 113:891–911

Malavel L, Liu F, Roche P, Aubin JE (1999) Kinetics of osteoprogenitor proliferation and osteoblast differentiation in vitro. J Cell Biochem 74:616–627

Raff MC, Durand B, Gao FB (1998) Cell number control and timing in animal development: the oligodendrocyte cell lineage. Int J Dev Biol 42:263–267

Tam PPL, Beddington RSP (1987) The formation of mesodermal tissues in the mouse embryo during gastrulation and early organogenesis. Development 99:109–126

Toole BP (1981) Gycosaminoglycans in morphogenesis. In: Hay E (ed) Cell biology of extracellular matrix. Plenum, New York, pp 259–294

Toole BP (1990) Hyaluronan and its binding proteins, the hyaladherins. Curr Opin Cell Biol 2:839–844

Winnier G, Blessing M, Labosky PA, Hogan BLM (1995) Bone morphogenetic protein-4 is required for mesoderm formation and patterning in the mouse. Genes Dev 9:2105–2116